



## Automated in-chip kinetic-catalytic method for molybdenum determination



Piyawan Phansi<sup>a,b</sup>, Camelia Henríquez<sup>c</sup>, Edwin Palacio<sup>c</sup>,  
Duangjai Nacapricha<sup>a,b</sup>, Víctor Cerdà<sup>c,\*</sup>

<sup>a</sup> Flow Innovation-Research for Science and Technology Laboratories (FIRST labs.), Thailand

<sup>b</sup> Department of Chemistry and Center of Excellence for Innovation in Chemistry, Faculty of Science, Mahidol University, Rama 6 Road, Bangkok 10400, Thailand

<sup>c</sup> Laboratory of Environmental Analytical Chemistry, University of the Balearic Islands, Carretera Valldemossa km 7.5, E-07122 Palma de Mallorca, Illes Balears, Spain

### ARTICLE INFO

#### Article history:

Received 3 September 2013

Received in revised form

17 October 2013

Accepted 22 October 2013

Available online 28 October 2013

#### Keywords:

Automation

Kinetic-catalytic

Spectrophotometry

Initial rate method

Integrated microconduit

Chip

### ABSTRACT

In this work, the automation of a catalytic spectrophotometric method for the determination of molybdenum is presented. For this purpose, a multisyringe flow injection system was coupled to an integrated microconduit that we have called “chip”. Reagents and sample were simultaneously dispensed to the chip where complete mixing, heating, and measurement were carried out. The spectrophotometric method is based on the oxidation of 4-amino-3-hydroxy-naphthalenesulphonic acid (AHNA) by hydrogen peroxide catalyzed by Mo (VI). Absorbance of the reaction product was measured at 465 nm. Two optical fibers were used to conduct the light, one from the source to the chip, and the other from the output of the cell to the spectrophotometer. The detection cell was incorporated in the thermostated zone of the chip. The initial rate method, at controlled temperature, was employed to determine the Mo (VI) concentration. The estimated precision was 3.7%, with the working range of 4.0–40  $\mu\text{g L}^{-1}$  of Mo (VI), and the limit of detection of 1.2  $\mu\text{g L}^{-1}$  of Mo (VI). The system was successfully applied to water samples and pharmaceutical products with a sampling throughput of 20 injections  $\text{h}^{-1}$ .

© 2013 Elsevier B.V. All rights reserved.

### 1. Introduction

Molybdenum (VI) is an essential trace element for plants and animals, including humans. In plants, this element is necessary to fix atmospheric nitrogen by bacteria to begin the protein synthesis. In animals, it is a component of xanthine oxidase and other redox enzymes. Molybdenum is also widely used in a variety of industrial processes such as metal alloys, pigments, lubricants and catalysts [1–3]. However, at high concentration molybdenum can be toxic to humans, plants and animals [2,4]. Most natural waters contain low levels of molybdenum in the range of  $< 2\text{--}3 \mu\text{g L}^{-1}$ , unless local anthropogenic sources have contaminated the waters [5]. The concentration of molybdenum in seawater is reported in the range of  $6\text{--}20 \mu\text{g L}^{-1}$  [3,6–8], and in mineral waters in the range of  $0.25\text{--}1.0 \mu\text{g L}^{-1}$  [9]. The U.S. EPA drinking water health advisories recommended long term limits of  $10 \mu\text{g L}^{-1}$  for children and  $50 \mu\text{g L}^{-1}$  for adults in daily drinking water, and the United Nations Food and Agriculture Organization recommends a maximum level for irrigation water of  $10 \mu\text{g L}^{-1}$  [10,11]. Therefore, the

development of a rapid, selective and sensitive method for determination of molybdenum is required.

There are a number of sensitive techniques for molybdenum determination in the  $\mu\text{g L}^{-1}$  range, such as spectrofluorimetry [12], voltammetry [13], inductively coupled plasma–mass spectrometry (ICP–MS) [5,14], inductively coupled plasma–atomic emission spectrometry (ICP–AES) [15,16], cloud point extraction and quantification by isotope dilution inductively coupled plasma mass spectrometry (CP/ICP–MS) [17] and electrothermal atomic absorption spectrometry (ETAAS) [9,18]. However, the need for pre-concentration and/or separation and the relatively high instrumental costs are disadvantages. Catalytic spectrophotometric methods offer low cost, simple and sensitive alternatives for the determination of trace levels of Mo (VI) [1,2,19–21].

There are some works using the initial rate method for catalytic determinations. Advantages of these methods are its wide working range, i.e. two or three orders of magnitude, and also its high sampling throughput [22,23]. However this method requires a strict control of the experimental conditions such as the mixture temperature in the detection cell and the measurement time. For that reason it is convenient to use automatic methods such as flow techniques to guaranty the reproducibility of the determination.

Flow techniques have some unique advantages, such as they do not require reaction to reach the equilibrium, and the use of very

\* Corresponding author.

E-mail address: [victor.cerda@uib.es](mailto:victor.cerda@uib.es) (V. Cerdà).

small sample and reagent volumes ( $\mu\text{L}$ ). They also provide sample throughput, low carry over, high degree of flexibility, and ease of automation. We have selected Multisyringe Flow Injection Analysis (MSFIA) as the flow-based technique since it includes the advantages of Flow Injection Analysis (FIA), in terms of mixing of flowing solutions, and of Sequential Injection Analysis (SIA) in relation to its robustness and versatility [24]. MSFIA is a low cost technique, which employs up to four syringes working in parallel as the liquid pumps. In this way, MSFIA overcomes some drawbacks of the peristaltic pumps, eliminates the presence of pulses, the needs of often recalibrations, and the corrosion effect of aggressive reagents and solvents. Moreover, MSFIA is computer controlled, and is therefore very well adapted for the stopped-flow technique. This technique also offers a reliable flow rate, unaffected by neither the flow resistance, nor sample viscosity. Therefore, MSFIA is a very appropriate technique for the kinetics method with homogeneous and highly reproducible mixing of the solutions, a critical requirement for this kind of determinations [25].

This work presents a multisyringe flow injection system coupled to a monolithic flow conduit, called Chip, for the automation of a catalytic spectrophotometric method. This chip was made of poly(methylmethacrylate) (PMMA). It integrated different steps of the analytical procedure such as: the confluent point, the mixing coil, the detection cell, all these on the thermostated chamber to control the temperature during the measurement step. This new device allowed the application of initial rate determination method at controlled temperature for the determination of molybdenum in waters and pharmaceutical samples.

## 2. Experimental

### 2.1. Reagents and standards

All chemicals were of analytical reagent grade. MilliQ water (Milli-Q plus,  $18.2 \text{ M}\Omega \text{ cm}^{-1}$ ) was employed for standard and reagent preparations.  $1000 \text{ mg L}^{-1}$  Mo (VI) stock standard solution was prepared by dissolving 1841 mg of ammonium heptamolybdate tetrahydrate ( $\text{Mo}_7\text{O}_{24}(\text{NH}_4)_6 \cdot 4\text{H}_2\text{O}$ ) (Scharlau, Spain) [26]. Working molybdenum standard solutions were prepared daily from their respective stocks. A  $0.0168 \text{ mol L}^{-1}$  4-amino-3-hydroxy-naphthalenesulfonic acid (AHNA) (Sigma-Aldrich, USA) was prepared, by dissolving 804 mg AHNA, 804 mg of  $\text{Na}_2\text{SO}_3$  (Fluka, Switzerland) and 102 mg of diethylenetriaminepentaacetic acid (DTPA) (Sigma-Aldrich, USA) in ca. 100 mL of water. The solution was then made up to 200 mL in a volumetric flask, and kept at room temperature [2,20]. The shelf life of the solution was 2 days. A  $0.42 \text{ mol L}^{-1}$  hydrogen peroxide ( $\text{H}_2\text{O}_2$ ) solution was prepared daily from a concentrated ( $9.79 \text{ mol L}^{-1}$ ) (Scharlau, Spain) solution. A  $0.48 \text{ mol L}^{-1}$  acetate buffer was prepared using 6.82 mL of  $17.60 \text{ mol L}^{-1}$  of acetic acid (Sigma-Aldrich, USA), adjusting pH to 5.00 with NaOH (suprapure Sigma-Aldrich, USA), and making up to volume in a 250 mL volumetric flask.

### 2.2. Reagents for the interference study

A stock solution of  $1000 \text{ mg L}^{-1}$  Fe (II) was prepared by dissolving 1404 mg of ammonium iron (II) sulfate 6-hydrate (Panreac, Spain) in water and made up to 20.0 mL. A stock  $1000 \text{ mg L}^{-1} \text{I}^-$  was prepared by dissolving 262 mg of potassium iodide (KI) (Scharlau, Spain) in water and made up to 20.0 mL. A stock  $1000 \text{ mg L}^{-1} \text{S}^{2-}$  was prepared by dissolving 1498 mg of sodium sulfide ( $\text{Na}_2\text{S} \cdot 9\text{H}_2\text{O}$ ) (ACROS Organics) in water and made up to 20.0 mL. Appropriate dilutions of these solutions were employed for the interference study. Appropriate dilution of Fe (III), Cr (VI), Mn (VII), and V (V) solutions were prepared from AAS

grade of stock  $1000 \text{ mg L}^{-1}$  Fe (III), Cr (VI), Mn (VII), and V (V), respectively (Scharlau, Spain).

### 2.3. Sample collection and preparation

One tablet of Hydropolivit is equivalent to  $100 \mu\text{g}$  of molybdenum (Hydropolivit  $1.91 \pm 0.02 \text{ g/tablet}$ ), whereas Multicentrum has  $50 \mu\text{g}$  of molybdenum per tablet (Multicentrum  $1.39 \pm 0.01 \text{ g/tablet}$ ).

For each product, 10 tablets were powdered in a mortar. Then 285 mg of the Hydropolivit and 417 mg of Multicentrum powder were accurately weighed, and transferred into 100 mL Teflon digestion vessels. 10 mL of ultrapure concentrated  $\text{HNO}_3$  (65%) (Scharlau, Spain) were added and the closed vessels, placed in a microwave oven (Milestone, START D) to digest the samples. The oven is equipped with a 2450 MHz microwave power supply of 0–1200 W output, a 6-position turntable and 100-mL Teflon liners with  $355^\circ$  rotatable pressure release valves, resistant up to 350 psi and  $210^\circ\text{C}$  (microwave program included in supporting information Table A-1). The digested solutions were cooled to room temperature and then evaporated to reduce their volume to a small drop. Finally, the volume was adjusted to 100 mL with MilliQ water to obtain a  $150 \mu\text{g L}^{-1}$  molybdenum solution. The pharmaceutical samples were filtered with  $0.45 \mu\text{m}$  cellulose acetate membrane (Sartorius Stedium Biotech, Germany) before analysis. A demolition leachate wastewater and several seawater samples were collected from different area of Mallorca (Balearic Islands, Spain). The water samples were filtered through a  $0.45 \mu\text{m}$  cellulose acetate membrane (Sartorius Stedium Biotech, Germany).

The ICP–AES technique was used as a reference method for the quantification of Mo (VI) in waters and pharmaceutical samples previously acidified with concentrated  $\text{HNO}_3$  (65%) (Scharlau, Spain) to 2%v/v. An ICP–AES (Optima 5300 DV, Perkin Elmer<sup>®</sup> Inc.) equipped with a Gem Tip Cross-flow pneumatic nebulizer (Waltham, MA, USA) was used under the following instrumental operating conditions: RF generator power 1300 W, frequency of RF generator 40 MHz, plasma argon flow  $15 \text{ L min}^{-1}$ , nebulizer argon flow  $0.8 \text{ L min}^{-1}$ , auxiliary argon flow  $0.5 \text{ L min}^{-1}$ , integration time 5 s and aspiration rate  $1.5 \text{ mL min}^{-1}$ . Wavelength for intensity measurements was 202.031 nm. All measurements were in triplicate.

### 2.4. Flow analyzer

The flow system is shown in Fig. 1. A multisyringe piston pump module (model Bu 4S) was purchased from Crison Instruments S.A. (Allela, Barcelona, Spain). The module was equipped with two 1 mL glass syringes (S3, and S4) and two 5 mL glass syringes of (S1, and S2). Solenoid valves (V1, V2, V3, and V4) allowed the connection of each syringe with either the chip (position ON, activated) or with the respective solution reservoir (position OFF, deactivated) for refilling. Solutions in the syringes were AHNA reagent in S1, Milli-Q water in S2,  $\text{H}_2\text{O}_2$  reagent in S3, and acetate buffer in S4. Furthermore, two external three-way solenoid valves (V5, V6) from Takasago (STV-3 1/4UKG, Nagoya, Japan) were powered and controlled using an auxiliary supply port of the multisyringe module. V5 was used for sample introduction (position ON). In position OFF V5 was connected to V6, and its common position was connected to a holding coil of 255 cm length and 1.00 mm i.d. which was connected to S2. V6 was used for introduction of air (position ON) which allowed the removal of small bubbles remaining inside the chip. All tubes of the flow system were of PTFE of 0.8 mm i.d.

The chip was constructed from three PMMA pieces,  $85 \times 44 \times 10 \text{ mm}^3$ , similar to that previously reported by Abouhiat et al. [25]. Threads of  $\frac{1}{4}$  in. 28 fittings were drilled in the upper part to connect the supply tubings for reagents and sample/carrier as well for the output of the integrated detection flow cell. On its

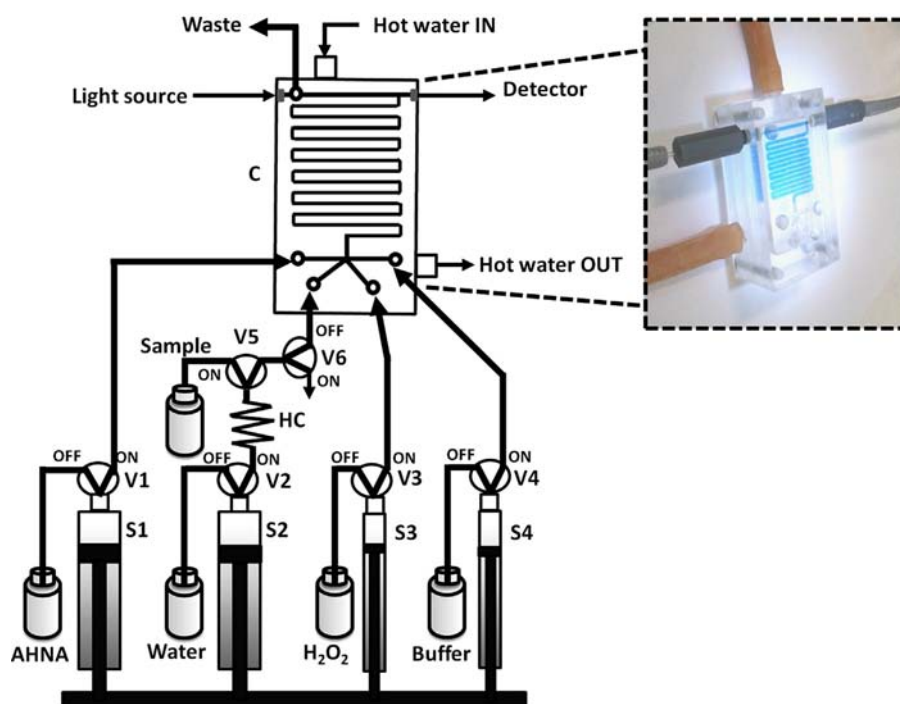


**Fig. 1.** Schematic diagram of the analytical system developed for the kinetic determination of molybdenum. S: syringe (S1 and S2: 5 mL, S3 and S4: 1 mL), V: solenoid valve, HC: holding coil of 255 cm and 1.00 mm id, C: PMMA chip, and detector: CCD miniature optical fiber spectrophotometer.

bottom side, a confluence and a serpentine reaction coil of  $0.8 \times 0.8 \times 39 \text{ mm}^3$  were made using a 3-axis PC controlled milling machine. In the lateral part two thread holes of UNF  $\frac{1}{4}$  in. 36 fittings were drilled in order to connect the optical fibers on the extreme ends of the final portion of the coil, as shown in Fig. 1. The middle piece was then glued to cover the flow circuit applying a thin film of methacrylic acid prior to tight fixation and a curing time of 1 h. In order to obtain a cavity below the flow circuit for the circulation of thermostat water, in the bottom piece, as well as in the already glued assembly, two rectangular deepening of  $50 \times 30 \times 8 \text{ mm}^3$  were milled prior to gluing both together. After curing, two flow connectors were attached to allow continuous flushing of the cavity with water from the thermostated bath (Selecta, Barcelona) via silicon tubes (ca. 20 cm, 1 cm id). The cavity served as a heating source to accelerate the reaction in the flow circuit. For sample analysis, a 45 position autosampler for 10 mL sample vials (Crison Instruments S.A., Barcelona, Spain) was placed at the sample tube. The multisyringe module and the autosampler were connected in series via a RS232C interface to a PC for remote software control (AutoAnalysis 5.0, Sciware Systems SL, Bunyola, Spain). A DH-2000 Deuterium light source (TOP Sensor Systems, Eerbeek, Netherlands) was used for providing the incident radiation, and an USB-2000 miniature CCD spectrophotometer (Ocean Optics Inc., Dunedin, FL, USA) was used as the detector. The reaction product was monitored at 465 nm.

### 2.5. Analytical protocol and flow method

The analytical procedure for the chip-MSFIA system is given in the supporting information (Table A-2). There are two parts: part one to remove bubbles, and part two to make measurements. The steps for removing bubbles (steps 1–3) were used to eliminate small bubbles produced during the reaction. These small bubbles could interfere with the measurement steps (affecting the reproducibility), and sometimes are quite difficult to remove. Therefore, a large air bubble was dispensed to remove the small bubbles

which remained in the chip. For the measurement steps, a 1.000 mL volume sample was aspirated from V5 (step 4), and then dispensed (step 5) for mixing and measuring in the chip. Absorbance of the reaction product was monitored at 465 nm at 20, 25, 30, 40, 45, 50, 55, and 60 s. The initial rate method, at a controlled temperature, was employed to determine the Mo (VI) concentration in the sample. Finally, the sample solution was dispensed to waste (step 7).

## 3. Results and discussion

The developed spectrophotometric method is based on the oxidation of 4-amino-3-hydroxy-naphthalenesulphonic acid (AHNA) with hydrogen peroxide, catalyzed by Mo (VI) [2,20]. The reagents and sample are simultaneously propelled to a chip where a complete mixing, thermostated and measurement is performed in a similar way as described elsewhere [25]. The main difference with respect to this paper is the integration of the detection flow cell in the chip. The absorbance of the reaction product is measured at 465 nm with an optical fiber spectrophotometer at various times in order to apply the initial-rate method. The calibration curve is obtained by plotting the slope of the kinetic curve vs the concentration of molybdenum.

### 3.1. Optimization of the experimental conditions

#### 3.1.1. Multivariate optimization

Fractionated two-level ( $2^{5-1}$ ) factorial design was used for screening of the effect of five different factors in the proposed method. The concentration of AHNA,  $\text{H}_2\text{O}_2$ , and HAc were kept within the ranges of 3–7  $\text{mmol L}^{-1}$ , 35–65  $\text{mmol L}^{-1}$ , and 30–50  $\text{mmol L}^{-1}$ , respectively. The pH of HAc was varied within the range of 5.0–5.6, and the temperature in the range of 45–55 °C. The data fitted well with a 2 way interaction model with a no significant lack of fit. Results (presented in supporting information Table A-3) indicated that interaction between HAc and pH,

concentration of AHNA, and temperature are significant and positive. The optimum conditions are for high temperature and low concentration of  $\text{H}_2\text{O}_2$ . From the screening analysis it can be inferred that the optimum values for each factor must be near  $55^\circ\text{C}$ ,  $7\text{ mmol L}^{-1}$  AHNA, and  $35\text{ mmol L}^{-1}\text{H}_2\text{O}_2$ , respectively.

Full factorial ( $3^2$ ) experimental design was used for optimization of concentration of HAC and pH (for  $55^\circ\text{C}$ ,  $7\text{ mmol L}^{-1}$  AHNA,  $35\text{ mmol L}^{-1}\text{H}_2\text{O}_2$ ) using an HAC experimental domain of  $20\text{--}40\text{ mmol L}^{-1}$ , and pH  $4.6\text{--}5.4$ . The data fitted well with 2-way interaction, without a significant lack of fit ( $r^2=0.999$ ), and a pure error of  $0.00003$  (see Supporting information Table S-2). This means that the pH and HAC have significant effects on the analytical signal.

However, the concentration of HAC has not significant effect in the studied range. The analysis of the marginal means indicated that the optimum pH value was 5.0 and concentration of HAC was  $40\text{ mmol L}^{-1}$  (see Supporting information, Fig. A-1).

The screening method also indicated that the selected temperature was the optimum condition. When the temperature is higher than  $55^\circ\text{C}$ , the blank signal increased and bubbles were produced interfering with the measurement. When the temperature was less than  $45^\circ\text{C}$ , both standard and blank signal decreased. Therefore, the concentration of AHNA and  $\text{H}_2\text{O}_2$  were studied in depth with a univariate procedure by fixing the temperature at  $55^\circ\text{C}$ , HAC at  $40\text{ mmol L}^{-1}$  and pH 5.0.

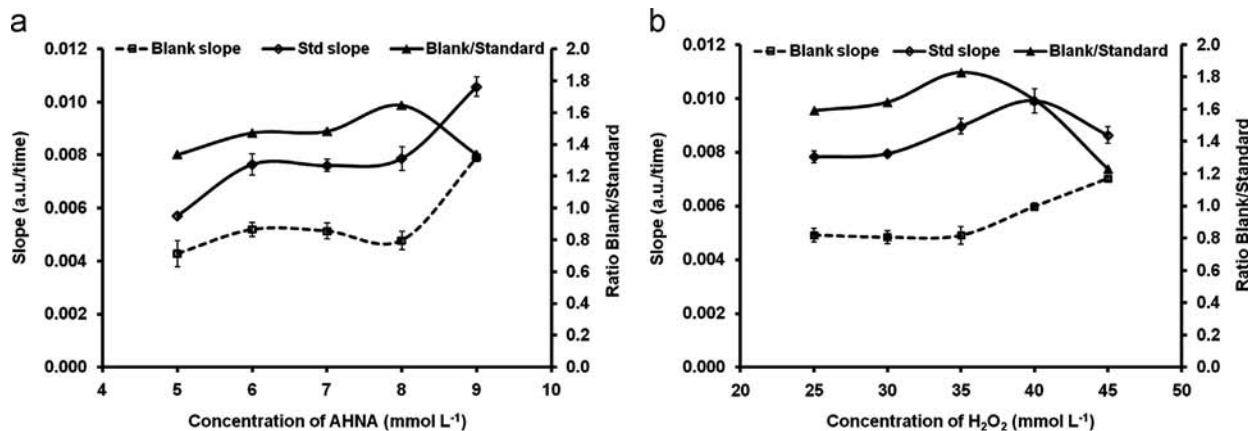


Fig. 2. Effects of AHNA (a) and  $\text{H}_2\text{O}_2$  (b) concentrations in the reaction initial rate. Experimental conditions:  $55^\circ\text{C}$ ,  $40\text{ mmol L}^{-1}$  HAC, pH 5.0, and  $35\text{ mmol L}^{-1}\text{H}_2\text{O}_2$  in (a), and  $7\text{ mmol L}^{-1}$  AHNA in (b). a.u.=absorbance units.

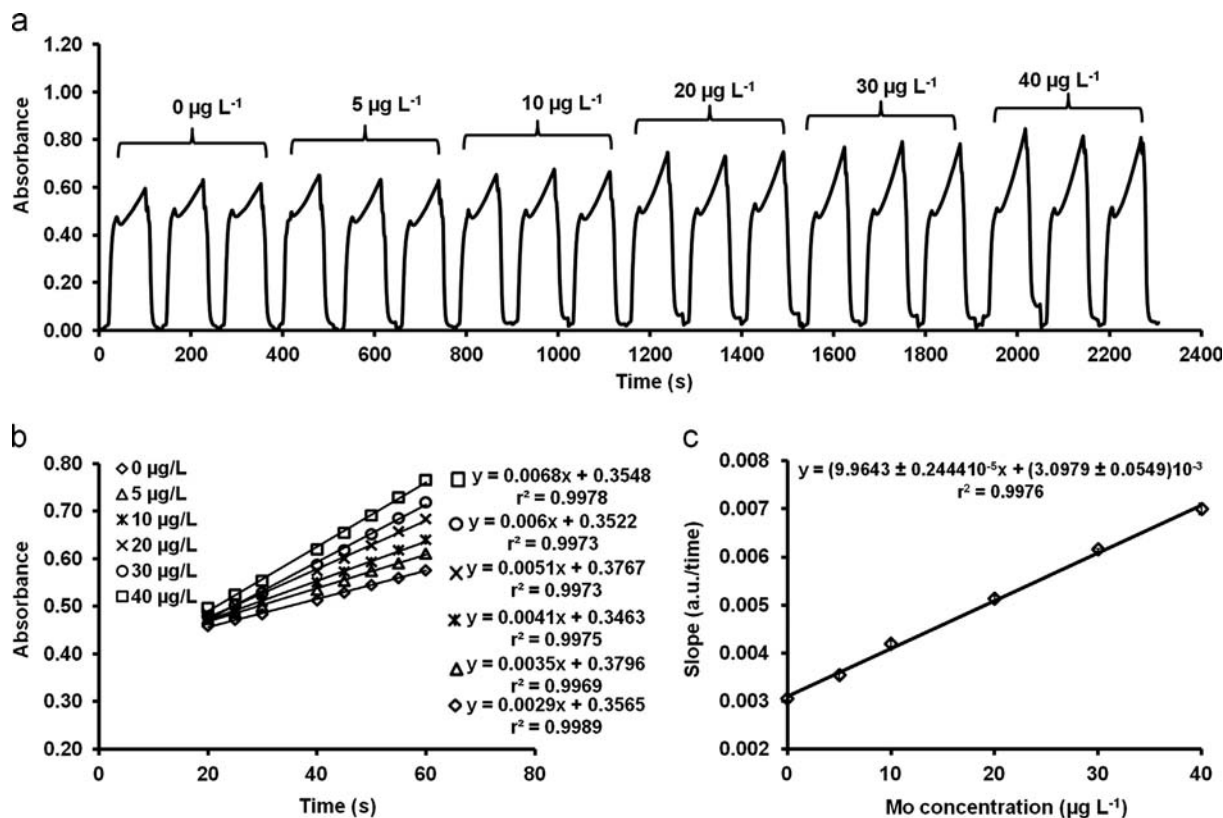


Fig. 3. (a) MSFIA-gram for the initial rate, (b) absorbance vs time curves, and (c) calibration curve obtained injecting different Mo (VI) standards under the optimum conditions,  $7\text{ mM}$  AHNA,  $35\text{ mM}$   $\text{H}_2\text{O}_2$ ,  $40\text{ mM}$  acetate buffer (pH 5.0), and temperature  $55^\circ\text{C}$ .



**Table 1**  
Figure of merit and experimental characteristics of spectrophotometric kinetic-catalytic Mo (VI) determination. Comparison with similar methods reported.

Ref.	Year	Reaction	$\lambda_{\max}$ (nm)	System	Method	Type of samples	Masking agent or separation	LOD ( $\mu\text{g L}^{-1}$ )	Working range ( $\mu\text{g L}^{-1}$ )	RSD, % ( $\mu\text{g L}^{-1}$ , n)	T (°C)	Throughput ( $\text{h}^{-1}$ )
[2]	2011	1-Amino-2-naphthol-4-sulfonic acid + $\text{H}_2\text{O}_2$	475	Batch	Fixed-time, 30 min	Natural and wastewater	DTPA	0.04	0.1–4.0		40	
[20]	2007	1-Amino-2-naphthol-4-sulfonic acid + $\text{H}_2\text{O}_2$	465	Batch	Fixed-time, 30 min	Natural and wastewater	DTPA	0.027	0–2.5		40	
[21]	2002	2-Aminophenol + $\text{H}_2\text{O}_2$	430	Batch	Fixed-time, 10 min	Natural and wastewater	EDTA	0.10	0–11.0	< 1.1% (–, n=5)	40	
[30]	2000	Nile blue A + hydrazine dihydrochloride	634	Batch	Fixed-time, 3 min	Plants: alfalfa and spinach	Cation exchanger resin	60	80–8000	1.6% (1000, n=10)	30	
[1]	2010	HBS ( $\text{HSO}_3(\text{C}_6\text{H}_4)_2\text{NHNH}_3^+$ ) is oxidized by bromate to p-sulfobenzendiazonium ion ( $\text{HSO}_3(\text{C}_6\text{H}_4)_2\text{N} \equiv \text{N}$ ) which is then coupled with NED to form a red azo dye	530	FIA	Fixed-time	Plant foodstuffs	Cation exchanger	0.50	1.0–20	2.5% (10, n=10)	60	15
[31]	1983	$\text{I}^- + \text{H}_2\text{O}_2$	350	FIA	Fixed-time	Natural and seawater	EDTA	0.7	20–120	2.3 (10, n=20)	25	90
Present work		1-Amino-2-naphthol-4-sulfonic acid + $\text{H}_2\text{O}_2$	465	Chip-MSFIA	Initial rate	Wastewater, tap water, seawater, and pharmaceutical samples	DTPA, NaF	1.2	4.0–40	3.72% (15, n=50)	55	20

### 3.1.2. Effect of AHNA concentration

The slopes of the catalyzed (with standard  $25 \mu\text{g L}^{-1}$  Mo) and the uncatalyzed reactions (blank) increased with the AHNA concentration. The maximum ratio between the slopes for the blank and standard was obtained for  $8 \text{ mmol L}^{-1}$  AHNA. However, for this value a lot of interfering bubbles were produced. Therefore a  $7 \text{ mmol L}^{-1}$  AHNA was chosen in the optimization of the concentration of  $\text{H}_2\text{O}_2$ , since the slopes of the standard and the blank for 6, 7, and 8 mM AHNA were not very different, as shown in Fig. 2(a).

### 3.1.3. Effect of $\text{H}_2\text{O}_2$ concentration

The univariate procedure was used to optimize the concentration of  $\text{H}_2\text{O}_2$  at  $55^\circ\text{C}$ ,  $40 \text{ mmol L}^{-1}$  HAC, pH 5.0, and  $7 \text{ mmol L}^{-1}$  AHNA, respectively. Results indicated that when the concentration of  $\text{H}_2\text{O}_2$  was increased, the slope of the standard also increased (Fig. 2(b)). However for AHNA, more than 35 mM, the slope of the blank also increased. Furthermore, when concentration of  $\text{H}_2\text{O}_2$  was more than 35 mM, there were a lot of interfering bubbles. Therefore a  $35 \text{ mmol L}^{-1}$   $\text{H}_2\text{O}_2$  concentration was chosen for further work.

### 3.2. Interference study

The effect of interfering ions on the determination of  $10 \mu\text{g L}^{-1}$  Mo was examined for the proposed method. The interfering ions, Fe (III), Fe (II),  $\text{S}^{2-}$ , V (V), Cr (VI), Mn (VII), and  $\text{I}^-$  were considered taking into account the results described by Mubarak et al. [20]. Results indicated that  $100 \mu\text{g L}^{-1}$  of both Fe (III) and Fe (II) produced a change in the slope of catalytic reaction less than 5%. However, at  $500 \mu\text{g L}^{-1}$  Fe (III) and Fe (II) produced a change in the slope of catalytic reaction of 9.46 and 7.73% respectively, and of concentration greater than  $500 \mu\text{g L}^{-1}$  Fe (III) and Fe (II) produced a change in the slope of catalytic reaction of more than 18%.  $\text{F}^-$  of  $0.2 \text{ mmol L}^{-1}$  could be successfully used for masking Fe (III). It has been reported that DTPA may be used to mask Fe (III) up to  $100 \mu\text{g L}^{-1}$  [20]. In our method we have used DTPA, but for samples containing higher concentration of Fe (III) it was necessary to add NaF to completely mask this interference. The proposed method has a tolerance for  $\text{S}^{2-}$  up to  $300 \mu\text{g L}^{-1}$  with a change in the slope of catalytic reaction less than 5%. However,  $700 \mu\text{g L}^{-1}$   $\text{S}^{2-}$  changes the slope by 15.4%. V (V), Cr (VI), and Mn (VII) did not interfere up to  $500 \mu\text{g L}^{-1}$ , and up to  $700 \mu\text{g L}^{-1}$  for  $\text{I}^-$  (maximum tested levels).

**Table 2**  
Mo (VI) quantification in seawater samples. Validation.

Samples	pH	Conductivity ( $\text{mS cm}^{-1}$ )	Proposed method		
			Added ( $\mu\text{g L}^{-1}$ )	Found $\pm$ S.D. ( $\mu\text{g L}^{-1}$ )	Recovery (%)
CRM (class 4) Seawater 1	7.42 8.10	40.4 46.5	0	$8.7 \pm 0.1$	
			5	$10.1 \pm 0.1$	
			10	$15.3 \pm 0.4$	104
			15	$19.6 \pm 0.2$	95
Seawater 2	7.98	45.4	0	$10.2 \pm 0.5$	
			5	$15.0 \pm 0.1$	96
			10	$20.6 \pm 1.0$	104
			15	$26.0 \pm 1.4$	105
Seawater 3	8.13	44.3	0	$9.7 \pm 0.1$	
			5	$14.9 \pm 0.4$	104
			10	$19.9 \pm 1.1$	102
			15	$25.2 \pm 0.4$	103
Seawater 4	8.10	45.1	0	$11.4 \pm 0.5$	
			5	$16.5 \pm 0.6$	102
			10	$21.7 \pm 0.7$	103
			15	$26.9 \pm 0.3$	103

These levels are considerably higher than those commonly found in the samples, (water and pharmaceutical samples).

### 3.3. Flow profile

Fig. 3(a) represent the MSFIA-gram obtained using the initial rate method for the reaction produced inside the chip and measured at 465 nm. Fig. 3(b) represents the absorbance values vs time used to calculate the slope of the initial rate [27,28]. Absorbance/time curves were obtained by injecting standards between 0 and 40  $\mu\text{g L}^{-1}$  Mo (VI) and measuring over the first minute of the reaction. Fig. 3(c) shows the calibration curve obtained from plotting the slope of the reaction vs the Mo (VI) standard concentration.

### 3.4. Analytical features

The analytical features of the flow system proposed in this paper are summarized in Table 1. The observed linear working range and LOD allow applying the proposed method for the Mo

(VI) quantification in water and pharmaceutical samples. There are other reported analytical methods based on molybdenum kinetic-catalytic redox reaction [29]. Some of these methods are summarized in Table 1 in order to compare them with our proposed method. Most are carried out as batch methods [2,20,21,30]. Although some of these batch methods are highly sensitivity, they are tedious and very time consuming. Only the method of Shigenori Nakano et al. [1] is automated using a FIA system for Mo (VI) determination in plants. However, it requires a cation exchanger to remove cation interferences. For this reason its detection limit is a bit better than our method at a cost of lower sample throughput and linear range. Zhao-Lun et al. [31] also present a FIA method which is based on the Mo (VI)-catalyzed iodide oxidation by hydrogen peroxide. This method presents relevant analytical features. However, it has higher number of interferences (tungstate, chromate and iron) than the chip-MSFIA method with ANHA (which only presents the interference of iron which can be easily masked with fluoride). Moreover, Zhao-Lun et al. [31] report a LOD of 0.7  $\mu\text{g L}^{-1}$  but they cannot quantified concentrations lower than 3  $\mu\text{g L}^{-1}$  and their calibration range lies

**Table 3**  
Mo (VI) quantification in pharmaceutical samples. Validation.

Samples	Proposed method				ICP-AES			Proposed method vs ICP-AES		Pharmaceutical reported Mo in medicine ( $\mu\text{g/pellet}$ )
	Spiked ( $\mu\text{g L}^{-1}$ )	Found $\pm$ S.D. ( $\mu\text{g L}^{-1}$ )	Recovery (%)	Mo in medicine ( $\mu\text{g/pellet}$ )	Spiked ( $\mu\text{g L}^{-1}$ )	Found $\pm$ S.D. ( $\mu\text{g L}^{-1}$ )	Mo in medicine ( $\mu\text{g/pellet}$ )	Found/ICP-AES Recovery (%)	t-obst-crit 95%=2.92	
Hydropolivit	0	16.2 $\pm$ 0.7		101.2 $\pm$ 3.0	0	15.9 $\pm$ 0.5	97.0 $\pm$ 2.9	102	0.35	100
	5	21 $\pm$ 1.1	96		5	20.8 $\pm$ 0.6		101	0.16	
	10	26 $\pm$ 1.1	98		10	25.4 $\pm$ 0.2		102	0.54	
	15	31.3 $\pm$ 0.8	101		15	31.8 $\pm$ 1.1		98	0.37	
Multicentrum	0	14.5 $\pm$ 0.4		48.4 $\pm$ 1.5	0	14.7 $\pm$ 0.1	49.1 $\pm$ 0.1	99	0.49	50
	5	19.5 $\pm$ 0.1	100		5	19.4 $\pm$ 0.3		101	0.32	
	10	25 $\pm$ 1.4	105		10	24.3 $\pm$ 0.6		103	0.46	
	15	30 $\pm$ 1.5	103		15	29.6 $\pm$ 1.3		101	0.20	

**Table 4**  
Mo (VI) quantification in wastewater samples. Validation.

Samples	pH	Conductivity ( $\mu\text{S cm}^{-1}$ )	Proposed method			ICP-AES		Proposed method vs ICP-AES	
			Added ( $\mu\text{g L}^{-1}$ )	Found $\pm$ S.D. ( $\mu\text{g L}^{-1}$ )	Spike-Recovery (%)	Added ( $\mu\text{g L}^{-1}$ )	Found $\pm$ S.D. ( $\mu\text{g L}^{-1}$ )	Found/ICP-AES Recovery (%)	t-obs t-crit 95%=2.92
Wastewater 1	7.54	1428	0	6.2 $\pm$ 0.2		0	6.0 $\pm$ 0.1	103	0.89
			5	11.3 $\pm$ 0.2	102	5	11.2 $\pm$ 0.5	101	0.19
			10	16.8 $\pm$ 0.1	106	10	16.2 $\pm$ 0.5	104	1.18
			15	21.3 $\pm$ 1.1	101	15	20.3 $\pm$ 1.2	105	0.61
Wastewater 2	7.87	1629	0	7.3 $\pm$ 0.1		0	7.1 $\pm$ 0.3	103	0.63
			5	12.3 $\pm$ 0.2	100	5	12.2 $\pm$ 0.3	101	0.28
			10	16.8 $\pm$ 0.2	95	10	16.9 $\pm$ 0.6	99	0.16
			15	23.3 $\pm$ 0.8	107	15	21.8 $\pm$ 1.8	107	0.76
Wastewater 3	7.71	1756	0	4.4 $\pm$ 0.3		0	4.0 $\pm$ 0.5	110	0.69
			5	9.5 $\pm$ 0.3	102	5	9.2 $\pm$ 0.1	103	0.95
			10	14.1 $\pm$ 0.5	97	10	13.8 $\pm$ 0.5	102	0.42
			15	20.2 $\pm$ 0.8	105	15	19.5 $\pm$ 0.2	104	0.85
Wastewater 4	8.04	1870	0	< LOD <sup>a</sup>		0	< LOD		
			5	5.2 $\pm$ 0.2	96	5	5.3 $\pm$ 0.3	98	0.55
			10	10.7 $\pm$ 0.4	103	10	10.2 $\pm$ 0.5	105	0.78
			15	16.7 $\pm$ 0.3	109	15	16.6 $\pm$ 0.3	101	0.24
Tap water	8.19	613	0	< LOD <sup>b</sup>		0	< LOD		
			5	5.8 $\pm$ 0.3	100	5	5.3 $\pm$ 0.5	109	0.86
			10	10.7 $\pm$ 0.5	99	10	10.0 $\pm$ 0.5	107	0.99
			15	16.1 $\pm$ 0.5	102	15	15.5 $\pm$ 0.4	104	0.94

These values are lower than the LOD, but they were taking into account because it was possible to differentiate them from the blank.

<sup>a</sup> It was used 0.4  $\mu\text{g L}^{-1}$  to calculate the spike-recovery percentage.

<sup>b</sup> It was used 0.8  $\mu\text{g L}^{-1}$  to calculate the spike-recovery percentage.

between 20 and 120  $\mu\text{g L}^{-1}$ . Additionally this method is not totally automated since they use a manual injection valve.

### 3.5. Validation and applications

According with IUPAC recommendation [32], the method has been validated using three independent tests: a certified reference material (Seawater CRM), a reference method (ICP–AES) and spiked samples (in three levels 5, 10 and 15  $\mu\text{g L}^{-1}$ ). As shown in Table 2, the proposed method can be used to quantify Mo (VI) in seawater samples, providing good results, both for a certified reference material, as well as for spiked samples. The Mo (VI) content in CRM (CASS-4, Nearshore Seawater Reference Material for Trace-Metals, Canada) obtained from chip-MSFIA method ( $8.7 \pm 0.1 \mu\text{g L}^{-1}$ ) agree well with CRM reported value ( $8.78 \pm 0.86 \mu\text{g L}^{-1}$ ). The recoveries for spiked samples lie between 95 and 104%. For pharmaceutical samples (Table 3), the Mo (VI) content obtained from the proposed method agree well with the value obtained using the reference method (ICP–AES), giving recoveries between 98 and 103%. Also the observed Mo (VI) value is not significantly different from the reported value for the pharmaceutical product ( $t\text{-obs} < t\text{-crit} = 2.92$ ). For waste and tap water samples with Mo (VI) content higher than 5  $\mu\text{g L}^{-1}$  the values agree well with those obtained with ICP–AES (Table 4). No significant different were found between these methods for a 95% confidence level of  $t$ -test ( $t\text{-obs} < t\text{-crit} = 2.92$ ), and the recovery of the comparison was between 98 and 110%. All these facts confirm the applicability of the proposed method to Mo (VI) determination in samples with high ionic strength. This could be related with the use of initial rate as the determination method. In this, the slope of the first instant of the kinetic curve is plotted vs [Mo (VI)] and for that reason, some optical effects such as the changes in the refraction index do not affect in the calibration.

## 4. Conclusions

The proposed automated system is a very simple, accurate, selective and sensitive method, which allows a reliable determination of Mo (VI) in very different complex matrices, like pharmaceuticals and water samples (wastewater, drink water, and seawater). This is the first time where a thermostated chip integrates the reaction manifold and the spectrophotometric flow cell, allowing the automation of the initial rate determination method. The initial rate method reduces the analysis time and tolerates high concentration of potential interfering ions. Furthermore, DTPA and NaF successfully mask Fe (III), which is the main interference ion in water and medicinal samples.

## Acknowledgments

The authors acknowledge the financial support from the Spanish Ministry of Science and Innovation through the project

CTQ2010-15541 and from the Conselleria d'Economia, Hacienda, e Innovació of the Government of the Balearic Islands through the allowance to competitive groups (43/2011) through Feder Funds. Scholarship from The Royal Golden Jubilee TRF-Ph. D. scholarship (for PP) is gratefully acknowledged.

## Appendix. Supplementary material

Supplementary data associated with this article can be found in the online version at <http://dx.doi.org/10.1016/j.talanta.2013.10.046>.

## References

- [1] S. Nakano, C. Kamaguchi, N. Hirakawa, *Talanta* 81 (2010) 786–791.
- [2] A.I. Mansouri, M. Mirzaei, D. Afzali, F. Ganjavie, *Arabian J. Chem.* (2013). (in press).
- [3] K. Pyrzynska, *Anal. Chim. Acta* 590 (2007) 40–48.
- [4] H. Filik, T. Çengel, R. Apak, *J. Hazard. Mater.* 169 (2009) 766–771.
- [5] D. Pozebon, V.L. Dressler, A.J. Curtius, *Talanta* 47 (1998) 849–859.
- [6] H.C. dos Santos, M.G.A. Korn, S.L.C. Ferreira, *Anal. Chim. Acta* 426 (2001) 79–84.
- [7] X. Huang, W. Zhang, G. Xu, S. Han, Y. Li, C. Li, *Talanta* 47 (1998) 869–875.
- [8] S.L. Costa Ferreira, H. Costa dos Santos, D. Santiago de Jesus, *Fresenius J. Anal. Chem.* 369 (2001) 187–190.
- [9] S.L.C. Ferreira, H.C. dos Santos, R.C. Campos, *Talanta* 61 (2003) 789–795.
- [10] E. Greenberg, L.S. Clesceri, A.D. Eaton, *Standard Method for the Examination of Water and Waste-Water*, American Public Health Association, Washington DC, 2000.
- [11] U.S. Environmental Protection Agency, *Drinking Water Regulations and Health Advisories*, EPA-822-B-002 U.S. EPA, Washington, D.C, 1996.
- [12] C. Jiang, J. Wang, F. He, *Anal. Chim. Acta* 439 (2001) 307–313.
- [13] A.A. Ensafi, S.S. Khaloo, *Talanta* 65 (2005) 781–788.
- [14] P. Cava-Montesinos, M.L. Cervera, A. Pastor, M. de la Guardia, *Anal. Chim. Acta* 531 (2005) 111–123.
- [15] K. Martynková, R. Komendová, M. Fišera, L. Sommer, *Microchim. Acta* 147 (2004) 65–71.
- [16] Y.K. Agrawal, K.R. Sharma, *Talanta* 67 (2005) 112–120.
- [17] A.C.S. Bellato, A.P.G. Gervasio, M.F. Giné, *J. Anal. At. Spectrom.* 20 (2005) 535–537.
- [18] J.L. Burguera, M. Burguera, C. Rondón, *Talanta* 58 (2002) 1167–1175.
- [19] D. Bejan, *Anal. Chim. Acta* 390 (1999) 255–259.
- [20] A.T. Mubarak, A.A. Mohamed, K.F. Fawy, A.S. Al-Shihry, *Talanta* 71 (2007) 632–638.
- [21] A.A. Mohamed, S.A. Ahmed, M.F. El-Shahat, *Monatsh. Chem.* 133 (2002) 31–40.
- [22] T. Tomiyasu, N. Teshima, S. Nakano, T. Kawashima, *Talanta* 47 (1998) 1093–1098.
- [23] T. Tomiyasu, *Anal. Chim. Acta* 312 (1995) 179–187.
- [24] B. Horstkotte, O. Elsholz, V. Cerdà, *J. Flow, Injection Anal.* 22 (2005) 99–109.
- [25] F.Z. Abouhiat, C. Henríquez, B. Horstkotte, F. El Yousfi, V. Cerdà, *Talanta* 108 (2013) 92–102.
- [26] A. Cara, J.M. Estela, R. Forteza, V. Cerdà, *Thermochim. Acta* 224 (1993) 271–279.
- [27] N. Rahman, N. Anwar, M. Kashif, *Chem. Pharm. Bull.* 54 (2006) 33–36.
- [28] S. Pervaiz, M.A. Farrukh, R. Adnan, F.A. Qureshi, *J. Saudi Chem. Soc.* 16 (2012) 63–67.
- [29] Z. Chen, N. Zhang, L. Zhuo, B. Tang, *Microchim. Acta* 164 (2009) 311–336.
- [30] M.F. Mousavi, A.R. Karami, *Microchem. J.* 64 (2000) 33–39.
- [31] F. Zhao-Lun, X. Shu-Kun, *Anal. Chim. Acta* 145 (1983) 143–150.
- [32] M. Thomson, S.L.R. Ellison, R. Wood, *Pure Appl. Chem.* 74 (2002) 835–855.